THE JOURNAL OF PHYSICAL CHEMISTRY A

Article

pubs.acs.org/JPCA

# Similarities and Differences between RNA and DNA Double-Helical Structures in Circular Dichroism Spectroscopy: A SAC−CI Study

Tomoo Miyahara[†] and Hiroshi Nakatsuji*[,†]

[†]Quantum Chemistry Research Institute, Kyodai Katsura Venture Plaza, North building 107, 1-36 Goryo-Oohara, Nishikyo-ku, Kyoto, 615-8245, Japan

Hiroshi Sugiyama[‡]

[‡]Department of Chemistry, Graduate School of Science, Kyoto University, Kitashirakawa-Oiwakecho, Sakyo-Ku, Kyoto 606-8502, Japan

Supporting Information

**ABSTRACT:** The helical structures of DNA and RNA are investigated experimentally using circular dichroism (CD) spectroscopy. The signs and the shapes of the CD spectra are much different between the right- and left-handed structures as well as between DNA and RNA. The main difference lies in the sign at around 295 nm of the CD spectra: it is positive for the right-handed B-DNA and the left-handed Z-RNA but is negative for the left-handed Z-DNA and the right-handed A-RNA. We calculated the SAC−CI CD spectra of DNA and RNA using the tetramer models, which include both hydrogen-bonding and stacking interactions that are important in both DNA and RNA. The SAC−CI results reproduced the features at around 295 nm of the experimental CD spectra of each DNA and RNA, and elucidated that the strong stacking interaction between the two base pairs is the origin of the negative peaks at 295 nm of the CD spectra for both DNA and RNA. On the basis of these facts, we discuss the similarities and differences between RNA and DNA double-helical structures in the CD spectroscopy based on the ChiraSac methodology.

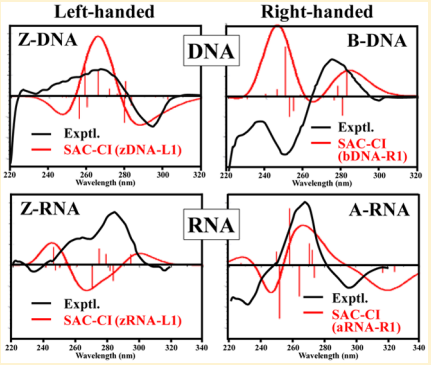


## 1. INTRODUCTION

DNA can form both right- and left-handed double-helical structures. The well-known double-helical structures include the right-handed A- and B-DNA and the left-handed Z-DNA. When DNA has a special sequence, the right-handed B-DNA transforms to the left-handed Z-DNA.[1−6] The transition from B- to Z-DNA or from Z- to B-DNA can be induced by the changes in salt concentration or temperature.[1−6] The left-handed Z-DNA is preferred at low temperature or at high salt concentration, but the right-handed B-DNA is preferred at the reverse conditions.[1−6]

The circular dichroism (CD) spectroscopy gives much information on the helical structure of DNA and RNA.[7,8] We can confirm whether the double-helical structure of a DNA at hand is right-handed or left-handed, because the CD spectra are much different between the B- and Z-DNA. For the CD spectra of B-DNA, the first (lowest) band has a positive sign and the second band has a negative sign, which is opposite to those of Z-DNA. When DNA changes from B- to Z-DNA, the negative peak appears at 295 nm in the CD spectra.[1−6] This is the feature of the CD spectra of Z-DNA.

RNA can also form both the right- and left-handed double-helical structures. The transition between the right-handed A-RNA and the left-handed Z-RNA can be induced by the changes in salt concentration or temperature.[9−11] These phenomena are quite similar to those of DNA. However, their CD spectra are opposite to those of DNA. For the CD spectra of the right-handed A-RNA, the first band at 295 nm has a negative sign and the second band has a positive sign,[9−11] which is the same feature as those of the left-handed Z-DNA. On the other hand, the features of the CD spectra of the left-handed Z-RNA are similar to those of the right-handed B-DNA. In addition, the right-handed A-RNA is preferred at low temperature,[9−11] similarly to the left-handed Z-DNA. Namely, the features of the CD spectra of RNA are opposite to those of DNA. However, for both DNA and RNA, the left-handed structures are preferred at high salt concentration.[1−6,9−11]

The helical structures of DNA were studied theoretically through its CD spectra with the time dependent density functional theory (Td-DFT)[12,13] and with the SAC−CI method.[14,15] We have studied the relationship between the helical structures of B- and Z-DNA and their CD spectra in the series of the ChiraSac studies using the SAC−CI method.[14,15] We showed that the hydrogen-bonding interaction tends to

**Received:** August 9, 2016
**Revised:** October 12, 2016
**Published:** October 19, 2016

ACS Publications © 2016 American Chemical Society



DOI: 10.1021/acs.jpca.6b08023
J. Phys. Chem. A 2016, 120, 9008−9018

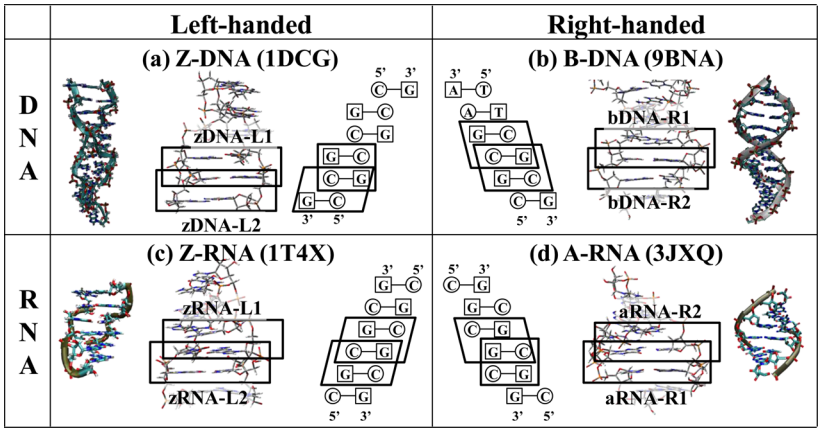


**Figure 1.** Tetramer models (zDNA-L1, zDNA-L2, bDNA-R1, bDNA-R2, zRNA-L1, zRNA-L2, aRNA-R1, and aRNA-R2) taken from the X-ray crystallographic structures of (a) Z-DNA (1DCG), (b) B-DNA (9BNA), (c) Z-RNA (1T4X) and (d) A-RNA (3JXQ). "G" and "C" represent guanine and cytosine, respectively.

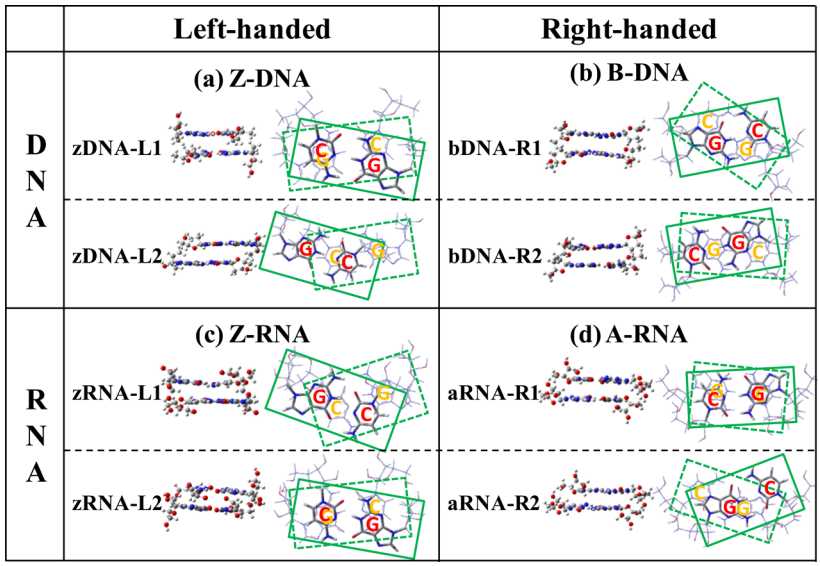


**Figure 2.** Side and top views of the tetramer models of (a) Z-DNA, (b) B-DNA, (c) Z-RNA, and (d) A-RNA. Squares of solid and dotted green lines represent the front-side and back-side base pairs, respectively. Red-colored "G" and "C" represent the front-side guanine and cytosine, respectively. Orange-colored "G" and "C" represent the back-side guanine and cytosine, respectively.

shift the excitation energies to higher values and that the stacking interaction changes the signs of the CD spectra.[14] In addition, we clarified that, in the CD spectra of Z-DNA, the negative sign of the first band originates from the strong stacking interaction inherent to its helical structure.[14,15]

We are developing a theoretical methodology, ChiraSac,[15−17] which is a theoretical molecular technology to study chiral molecular systems with a combined use of the SAC−CI method[18−26] and other useful methods present in the Gaussian suite of programs[27] to investigate the chemical and biological weak interaction phenomena through their CD and UV spectra. Detailed explanations of the "ChiraSac" were presented before.[15−17] In this paper, we perform a comparative ChiraSac study of DNA and RNA: we calculate the SAC−CI CD and UV spectra of DNA and RNA to clarify the relationship between the helical structures and their CD spectra, and to elucidate the similarities and differences between DNA and RNA.

## 2. MODELING

The geometries were taken from the X-ray crystallographic structures: 1DCG, 9BNA, 1T4X and 3JXQ were used for Z-DNA, B-DNA, Z-RNA and A-RNA, respectively, as shown in Figure 1a−d. These structures have the same sequence in which deoxyguanosine (dG) and deoxycytidine (dC) for DNA and guanosine (G) and cytidine (C) for RNA are arranged alternately. We labeled the models 1 of the left-handed Z-DNA as zDNA-L1 (*Z-DNA L*eft-handed model *1*) and model 2 of the right-handed A-RNA as aRNA-R2 (*A-RNA R*ight-handed model *2*), etc. We calculated the CD and UV spectra of Z- and B-DNA and Z- and A-RNA using the tetramer models (see Figure 1) as used in the previous paper.[14,15] The geometries of the hydrogen atoms attached by the GaussView were optimized by the B3LYP[28,29]/6-31G(d,p)[30,31] for the DNA model, but were used without optimization for RNA. The coordinates of the eight tetramer models are shown in Supporting Information, Tables S1−S8.

We calculated two tetramer models for each DNA or RNA. Parts a−d of Figures 2 show the side and top views of the



DOI: 10.1021/acs.jpca.6b08023
J. Phys. Chem. A 2016, 120, 9008−9018

**Table 1. Average, Maximum, and Minimum Distances between the Two Base Pairs (Å)**

| | DNA | | | | RNA | | | |
|---|---|---|---|---|---|---|---|---|
| | left-handed Z-DNA | | right-handed B-DNA | | left-handed Z-RNA | | right-handed A-RNA | |
| | zDNA-L1 | zDNA-L2 | bDNA-R1 | bDNA-R2 | zRNA-L1 | zRNA-L2 | aRNA-R1 | aRNA-R2 |
| average | 3.525 | 3.438 | 3.605 | 3.332 | 3.436 | 3.167 | 3.316 | 2.922 |
| maximum | 4.097 | 3.788 | 4.715 | 4.067 | 4.560 | 3.542 | 4.374 | 3.882 |
| minimum | 3.256 | 3.140 | 2.486 | 2.588 | 2.536 | 2.658 | 2.351 | 1.552 |
| Δ[a] | 0.841 | 0.648 | 2.229 | 1.479 | 2.024 | 0.884 | 2.023 | 2.330 |
| average of Δ | 0.745 | | 1.854 | | 1.454 | | 2.177 | |

[a]Δ = maximum distance − minimum distance.

tetramer models for Z-DNA, B-DNA, Z-RNA, and A-RNA, respectively. The hydrogen-bonding base pairs of each tetramer model are shown by the squares of the solid and dotted green lines. For the zDNA-L1, zRNA-L2 and aRNA-R1 models, the overlap between the two squares is large. Namely, the purine ring of guanine has a large overlap with the pyrimidine ring of cytosine. However, for the other models, the overlap between the two squares is not large: either the purine or the pyrimidine ring of the back-side base pair is situated in the region between guanine and cytosine of the front-side base pair. Therefore, from Figure 2, we can estimate that the zDNA-L1, zRNA-L2, and aRNA-R1 models have the strong stacking interaction due to the large overlap between the two base pairs.

Table 1 shows the average, maximum, and minimum distances between the two base pairs of the eight tetramer models. For DNA, the average distance is similar between the right- and left-handed structures. However, for RNA, the average distance is shorter for the right-handed A-RNA than for the left-handed Z-RNA. The Δ (the difference between maximum and minimum distances) increases in the order of Z-DNA, Z-RNA, B-DNA, and A-RNA. When we compare the double-helical structures of the four types of nucleic acids, the two base pairs are approximately parallel for Z-DNA, but one base pair is largely inclined from the other base pair for A-RNA.

Table 2 shows the angles between the two bases of each model: they were taken from the X-ray crystallographic structures. As shown in Figure 3, the quantities h1, h2, and h3 represent the angles between the two bases in the hydrogen-bonding base pair and s1, s2, s3, and s4 represent the angles between the two bases in the stacking base pair in the models 1 and 2. The angle =0° means that the two bases are parallel to each other, but the angle =90° means that the two bases are perpendicular to each other. In all hydrogen-bonding and stacking base pairs, one base is inclined from the other base. However, the angles between the two bases are small in Z-DNA, but large in B-DNA, Z-RNA, and A-RNA, showing that the two base pairs of Z-DNA are relatively parallel as compared with the others. Namely, combined with the fact from Figure 2 that the zDNA-L1, zRNA-L2, and aRNA-R1 models have the large overlap between the two base pairs, the stacking interaction is estimated to be strongest in the zDNA-L1 model.

**Table 2. Angles between the Two Bases (deg)[a]**

| | DNA | | RNA | |
|---|---|---|---|---|
| angle[b] | Z-DNA | B-DNA | Z-RNA | A-RNA |
| h1 | 4.7 | 8.2 | 13.1 | 10.6 |
| h2 | 7.3 | 6.5 | 6.1 | 9.6 |
| h3 | 1.9 | 13.1 | 3.7 | 10.5 |
| s1 | 7.2 | 15.5 | 10.1 | 7.6 |
| s2 | 3.1 | 11.5 | 9.0 | 8.1 |
| s3 | 2.6 | 4.3 | 9.4 | 11.6 |
| s4 | 7.3 | 9.3 | 7.2 | 12.3 |
| ave. | 4.9 | 9.8 | 8.4 | 10.0 |

[a]Angle =0° means that the two bases are parallel to each other. Angle =90° means that the two bases are perpendicular to each other. [b]The h1, h2 and h3 represent the angle between the two bases in the hydrogen-bonding base pair and the s1, s2, s3 and s4 represent the angle between the two bases in the stacking base pair, in the models 1 and 2 shown in Figure 3.

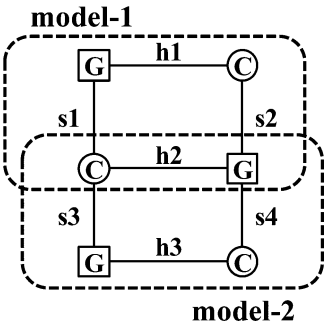


**Figure 3.** Definition of the angles (h1, h2, h3, s1, s2, s3, and s4) between the two bases used in Table 2. "G" and "C" represent guanine and cytosine, respectively. Model-1 means zDNA-L1, bDNA-R1, zRNA-L1 and aRNA-R1. Model-2 means zDNA-L2, bDNA-R2, zRNA-L2 and aRNA-R2.

## 3. COMPUTATIONAL DETAILS

In the SAC/SAC−CI calculations, the double-ζ plus polarization basis sets are necessary for the calculations of the CD spectra of DNA.[14,15] However, because of the high computational cost, the basis functions employed were D95(d)[32] for the nucleic acid bases and D95[32] for deoxyribose of DNA and ribose of RNA, and the core orbitals of C, O and N atoms were treated as frozen orbitals. All single and selected double excitation operators were included and perturbation selection[33] was carried out with the threshold sets of LevelThree. As the active orbitals, we included the MO's whose energies were within −1.20 to +1.20 au for the DNA models and within −1.20 to +1.10 au for the RNA models. The calculated SAC−CI UV and CD spectra were convoluted using the Gaussian envelopes to describe the Franck−Condon widths and the resolution of the spectrometer. The full width at half-maximum (fwhm) of the Gaussian envelope was taken to be 0.4 eV for both SAC−CI UV and CD spectra. The rotatory strengths ($R_{0a}$) of CD spectra were calculated using the gauge-invariant velocity form given by


DOI: 10.1021/acs.jpca.6b08023
J. Phys. Chem. A 2016, 120, 9008−9018

**Table 3. Excited States of zDNA-L1 Model**

| | SAC−CI | | | | | | exptl (eV/nm) | |
|---|---|---|---|---|---|---|---|---|
| state | EE (eV)[a] | EE (nm)[a] | osc[b] | rot[c] | nature[d] | type[e] | CD[f] | UV[g] |
| $1^1$A | 4.60 | 270 | 0.003 | −16.91 | $\pi_{g,h} \rightarrow \pi_{c,l}^*$ | ET(s) | 4.20/295 | |
| $2^1$A | 4.69 | 264 | 0.005 | −5.72 | $\pi_{g,h} \rightarrow \pi_{c,l}^*$ | ET(s) | 4.20/295 | |
| $3^1$A | 4.88 | 254 | 0.010 | −45.70 | $\pi_{g,h} \rightarrow \pi_{g,l}^*$ | dG | 4.20/295 | |
| $4^1$A | 4.92 | 252 | 0.191 | 72.61 | $\pi_{c,h} \rightarrow \pi_{c,l}^*$ | dC | | 4.28/290 |
| $5^1$A | 4.93 | 252 | 0.053 | −129.87 | $\pi_{c,h} \rightarrow \pi_{c,l}^* + \pi_{c,h-1} \rightarrow \pi_{c,l}^*$ | dC | 4.20/295 | 4.28/290 |
| $6^1$A | 4.99 | 248 | 0.053 | 12.25 | $\pi_{g,h} \rightarrow \pi_{g,l}^* + \pi_{c,h-1} \rightarrow \pi_{c,l}^*$ | dG + dC | | 4.28/290 |
| $7^1$A | 5.06 | 245 | 0.014 | 35.45 | $\pi_{c,h-1} \rightarrow \pi_{c,l}^* + \pi_{c,h} \rightarrow \pi_{c,l}^*$ | dC | | |
| $8^1$A | 5.16 | 240 | 0.541 | 121.83 | $\pi_{c,h-1} \rightarrow \pi_{c,l}^*$ | dC | 4.63/268 | 4.84/256 |
| $9^1$A | 5.27 | 235 | 0.034 | −54.55 | $n_g \rightarrow \pi_{g,l}^*$ | dG | | |
| $10^1$A | 5.29 | 234 | 0.415 | 138.46 | $\pi_{g,h} \rightarrow \pi_{g,l+1}^*$ | dG | 4.63/268 | 4.84/256 |
| $11^1$A | 5.35 | 232 | 0.303 | −109.38 | $\pi_{g,h} \rightarrow \pi_{g,l+1}^*$ | dG | | 4.84/256 |
| $12^1$A | 5.43 | 228 | 0.004 | −5.28 | $n_c \rightarrow \pi_{c,l}^*$ | dC | | |
| $13^1$A | 5.48 | 226 | 0.003 | −7.85 | $n_c \rightarrow \pi_{c,l}^*$ | dC | | |
| $14^1$A | 5.52 | 225 | 0.005 | −6.09 | $n_g \rightarrow \pi_{g,l+1}^*$ | dG | | |

[a]Excitation energy. [b]Oscillator strength. [c]Rotatory strength ($10^{-40}$ cgs). [d]Subscript *g* and *c* represent guanine and cytosine, respectively. Subscripts *h*, *h*−*1*, *l*, and *l*+*1* represent the highest occupied molecular orbital (HOMO), HOMO−1, the lowest unoccupied molecular orbital (LUMO), and LUMO+1 of dG or dC. [e]dG and dC represent the intramolecular excited states of deoxyguanosine and deoxycytidine, respectively. ET(s) represents the electron transfer excited states from guanine to cytosine through the stacking interaction. [f]Reference 6 [g]Reference 2.

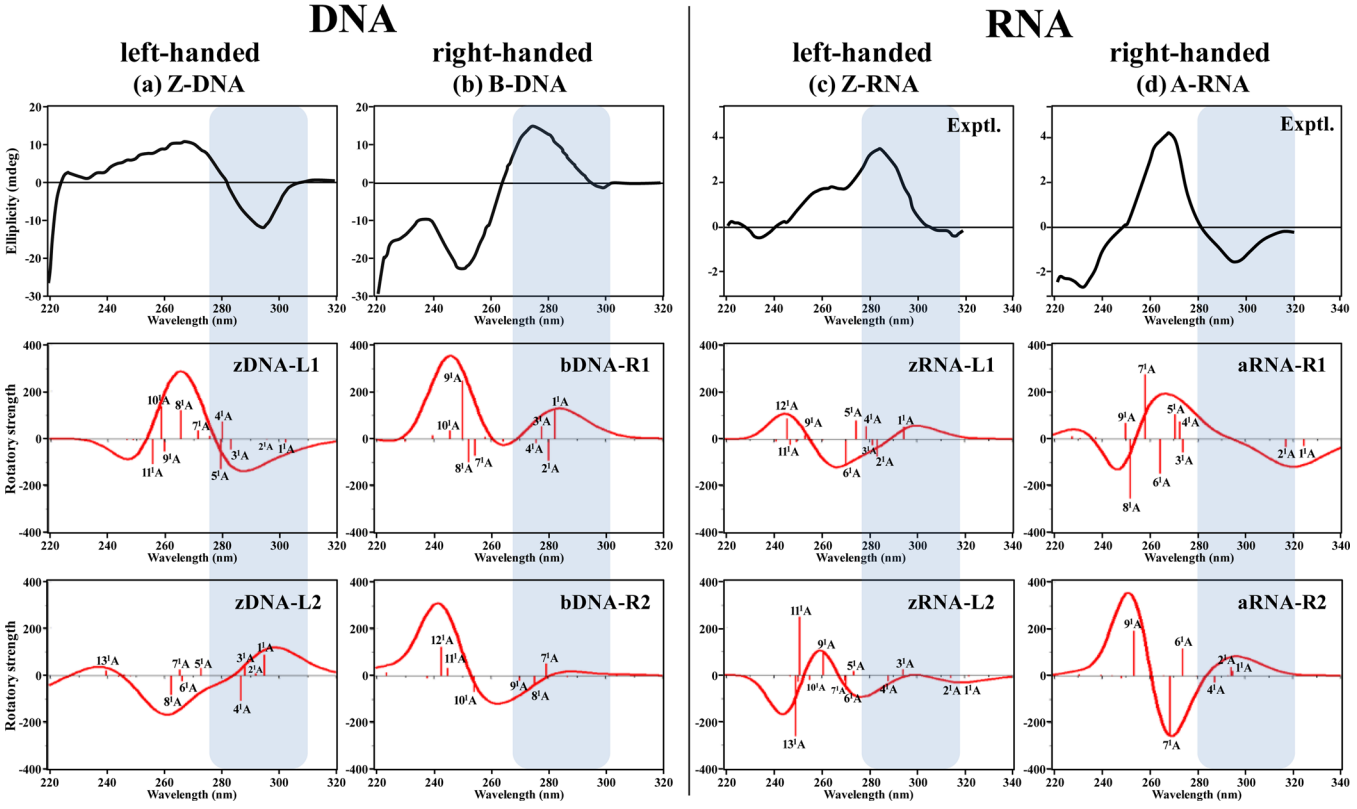


**Figure 4.** SAC−CI CD spectra (red lines) of the eight tetramer models as compared with the experimental CD spectra (black lines).[6,11] All excited states of SAC−CI calculations have been shifted to the lower sides by the values of 0.5 eV for DNA and 0.7 eV for RNA from the excitation energies of Tables 3−10, respectively. Blue-colored squares represent the first band region of the CD spectra of each DNA or RNA.

$$R_{0a} = \mathrm{Im}\left\{\frac{\langle\Psi_0|\nabla|\Psi_a\rangle\langle\Psi_a|\hat{m}|\Psi_0\rangle}{E_a - E_0}\right\} \quad (1)$$

## 4. SAC−CI CD SPECTRA

Tables 3−10 show the excitation energies, oscillator strengths, rotatory strengths, natures, and types of the excited states of the SAC−CI results for the eight tetramer models (see Section 6 below for the detailed explanations). In order to compare the experimental CD spectra, it is necessary to shift the present SAC−CI results to the lower sides by the values of 0.5 eV for DNA and 0.7 eV for RNA, since we cut the active space windows of SAC−CI to much smaller ones to save the computer time as explained in the previous section 3, "Computational details". Figures 4 (a) to (d) show the SAC−CI CD spectra of the two tetramer models for Z-DNA,


DOI: 10.1021/acs.jpca.6b08023
J. Phys. Chem. A 2016, 120, 9008−9018

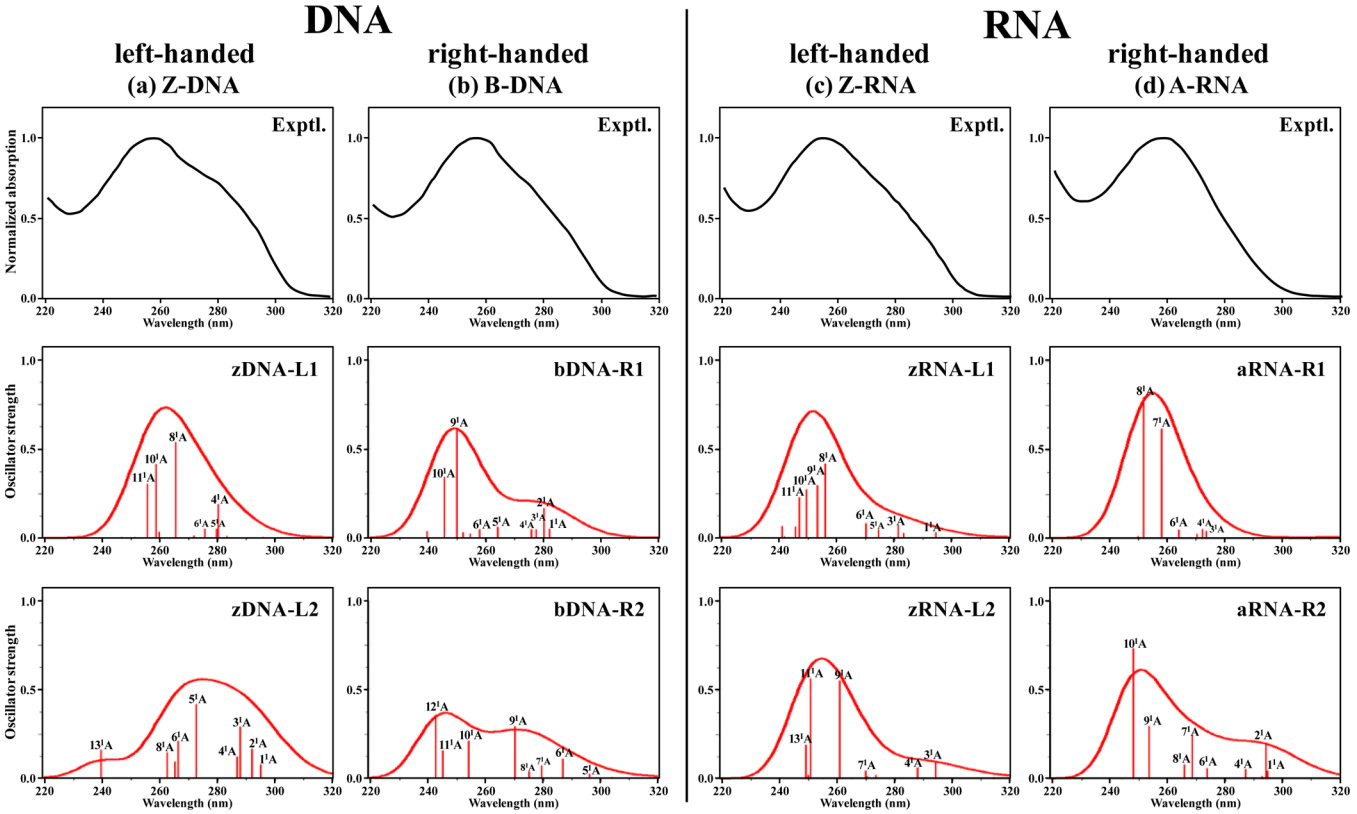


**Figure 5.** SAC−CI UV spectra (red lines) of the eight tetramer models as compared with the experimental UV spectra (black lines).[2,9] All excited states of SAC−CI calculations have been shifted to the lower sides by the values of 0.5 eV for DNA and 0.7 eV for RNA from the excitation energies of Tables 3−10, respectively.

B-DNA, Z-RNA and A-RNA, respectively, compared with their experimental CD spectra measured in water solution.[6,11]

The SAC−CI CD spectra seemed to be not in good agreement with the experimental CD spectra at first glance. However, the SAC−CI CD spectra of the zDNA-L1 and aRNA-R1 models were in good correspondence with the experimental CD spectra of Z-DNA and A-RNA, respectively. But the SAC−CI CD spectra of the zDNA-L2 and aRNA-R2 models were opposite to those of the zDNA-L1 and aRNA-R1 models. Even though the tetramer models taken from the same helical structures were used, the negative peak did not appear at 295 nm in the CD spectra unless the overlap between the two base pairs was large. Namely, the negative peak is observed at 295 nm due to the large overlap between the two base pairs, in other words, due to the strong stacking interaction. Therefore, the peak at 295 nm can become the indicator of the strong stacking interaction for the double-helical structures of DNA as well as RNA.[14,15]

On the other hand, for the SAC−CI CD spectra of the bDNA-R1 and zRNA-L1 models, the sign of the lowest band was the same as that of the experiment, but their shapes were much different from the experimental CD spectra in a high-energy region. The SAC−CI CD spectra of the bDNA-R2 and zRNA-L2 models are quite different from the experimental CD spectra. Since Z-DNA and A-RNA are preferred at low temperature but B-DNA and Z-RNA are preferred at high temperature, B-DNA and Z-RNA are less stable and more flexible than Z-DNA and A-RNA. Actually, the angles (s1 and s2) between the two bases in the stacking base pair are larger for the bDNA-R1 and zRNA-L1 models than for the zDNA-L1 and aRNA-R1 models, respectively (see Table 2). This shows that the stacking interaction is weaker in B-DNA and Z-RNA than in Z-DNA and A-RNA.

## 5. SAC−CI UV SPECTRA

Parts a−d of Figure 5 show the SAC−CI UV spectra of the two tetramer models for Z-DNA, B-DNA, Z-RNA, and A-RNA, respectively, compared with their experimental UV spectra measured in water solution.[2,9] The SAC−CI UV spectra were similar among all models as compared with the SAC−CI CD spectra, since only the $\pi \rightarrow \pi^*$ excited states within the nucleic acid bases have a strong oscillator strength. However, since the ground state of the bDNA-R2 model was unstable, its excitation energies were calculated to be lower than those of other models (see Table 6). In the experimental UV spectra, the shoulder peak at 280 nm is stronger for the left-handed Z-DNA and Z-RNA than for the right-handed B-DNA and A-RNA. The shoulder peak is also slightly observed for B-DNA, but is not observed for A-RNA. As explained in the next section, the shoulder peak is due to the intramolecular excitation within the nucleic acid bases. However, the lowest intramolecular excitation of the aRNA-R1 model was calculated to be at a higher energy region than those of the other models (see Table 9). Therefore, the shoulder peak did not exist for the aRNA-R1 model.

## 6. DETAILED NATURES OF THE EXCITED STATES

**6.1. Z-DNA (Tables 3 and 4).** The behaviors of the experimental CD spectrum of Z-DNA, being negative for the first band and positive for the second band, are in good agreement with those of the SAC−CI CD spectrum of the



DOI: 10.1021/acs.jpca.6b08023
J. Phys. Chem. A 2016, 120, 9008−9018

**Table 4. Excited States of zDNA-L2 Model**

| | SAC−CI | | | | | | exptl (eV/nm) | |
|---|---|---|---|---|---|---|---|---|
| state | EE (eV)[a] | EE (nm)[a] | osc[b] | rot[c] | nature[d] | type[e] | CD[F] | UV[g] |
| $1^1$A | 4.70 | 264 | 0.076 | 86.41 | $\pi_{g,h} \rightarrow \pi_{g,l}^*$ | dG | − | |
| $2^1$A | 4.74 | 261 | 0.165 | 8.53 | $\pi_{c,h} \rightarrow \pi_{c,l}^*$ | dC | | 4.28/290 |
| $3^1$A | 4.80 | 258 | 0.291 | 46.95 | $\pi_{c,h} \rightarrow \pi_{c,l}^*$ | dC | | 4.28/290 |
| $4^1$A | 4.82 | 257 | 0.122 | −109.81 | $\pi_{g,h} \rightarrow \pi_{g,l}^*$ | dG | | 4.28/290 |
| $5^1$A | 5.04 | 246 | 0.417 | 31.20 | $\pi_{g,h} \rightarrow \pi_{g,l+1}^*$ | dG | | 4.84/256 |
| $6^1$A | 5.15 | 241 | 0.210 | −26.19 | $\pi_{g,h} \rightarrow \pi_{g,l+1}^* + \pi_{g,h} \rightarrow \pi_{c,l}^*$ | dG + ET(s) | | 4.84/256 |
| $7^1$A | 5.17 | 240 | 0.094 | 24.04 | $\pi_{g,h} \rightarrow \pi_{c,l}^* + \pi_{g,h} \rightarrow \pi_{g,l+1}^*$ | ET(s) + dG | | |
| $8^1$A | 5.22 | 237 | 0.145 | −84.65 | $\pi_{c,h-1} \rightarrow \pi_{c,l}^*$ | dC | | 4.84/256 |
| $9^1$A | 5.50 | 226 | 0.001 | −4.79 | $n_g \rightarrow \pi_{g,l}^*$ | dG | | |
| $10^1$A | 5.54 | 224 | 0.003 | 3.37 | $n_g \rightarrow \pi_{c,l}^*$ | ET(h) | | |
| $11^1$A | 5.56 | 223 | 0.002 | −1.66 | $n_g \rightarrow \pi_{c,l}^*$ | ET(h) | | |
| $12^1$A | 5.58 | 222 | 0.001 | −6.36 | $n_g \rightarrow \pi_{g,l+1}^*$ | dG | | |
| $13^1$A | 5.67 | 219 | 0.160 | 21.39 | $\pi_{c,h-1} \rightarrow \pi_{c,l}^*$ | dC | | |
| $14^1$A | 6.27 | 198 | 0.006 | −20.95 | $n_g \rightarrow \pi_{g,l+1}^*$ | dG | | |

[a]Excitation energy. [b]Oscillator strength. [c]Rotatory strength ($10^{-40}$ cgs). [d]Subscript *g* and *c* represent guanine and cytosine, respectively. Subscripts *h*, *h*−*1*, *l*, and *l*+*1* represent the highest occupied molecular orbital (HOMO), HOMO−1, the lowest unoccupied molecular orbital (LUMO), and LUMO+1 of dG or dC. [e]dG and dC represent the intramolecular excited states of deoxyguanosine and deoxycytidine, respectively. ET(s) and ET(h) represent the electron transfer excited states from guanine to cytosine through the stacking and hydrogen-bonding interactions, respectively. [F]Not assigned. [g]Reference 2.

**Table 5. Excited States of bDNA-R1 Model**

| | SAC−CI | | | | | | exptl (eV/nm) | |
|---|---|---|---|---|---|---|---|---|
| state | EE (eV)[a] | EE (nm)[a] | osc[b] | rot[c] | nature[d] | type[e] | CD[f] | UV[g] |
| $1^1$A | 4.89 | 254 | 0.051 | 123.69 | $\pi_{g,h} \rightarrow \pi_{g,l}^*$ | dG | 4.49/276 | |
| $2^1$A | 4.92 | 252 | 0.168 | −95.75 | $\pi_{c,h} \rightarrow \pi_{c,l}^*$ | dC | | 4.28/290 |
| $3^1$A | 4.96 | 250 | 0.049 | 52.79 | $\pi_{c,h} \rightarrow \pi_{c,l}^*$ | dC | 4.49/276 | |
| $4^1$A | 4.99 | 248 | 0.048 | −18.45 | $\pi_{g,h} \rightarrow \pi_{c,l}^*$ | ET(s) | | |
| $5^1$A | 5.19 | 239 | 0.064 | −12.44 | $\pi_{g,h} \rightarrow \pi_{g,l}^*$ | dG | | |
| $6^1$A | 5.30 | 234 | 0.049 | 8.54 | $\pi_{c,h-1} \rightarrow \pi_{c,l}^*$ | dC | | |
| $7^1$A | 5.37 | 231 | 0.025 | −74.58 | $n_c \rightarrow \pi_{c,l}^*$ | dC | 4.96/250 | |
| $8^1$A | 5.41 | 229 | 0.033 | −101.60 | $\pi_{g,h} \rightarrow \pi_{c,l}^*$ | ET(s) | 4.96/250 | |
| $9^1$A | 5.46 | 227 | 0.619 | 246.91 | $\pi_{g,h} \rightarrow \pi_{g,l+1}^*$ | dG | | 4.84/256 |
| $10^1$A | 5.55 | 224 | 0.344 | 35.30 | $\pi_{g,h} \rightarrow \pi_{g,l+1}^*$ | dG | | 4.84/256 |
| $11^1$A | 5.67 | 219 | 0.039 | 13.62 | $n_{c+g} \rightarrow \pi_{c,l}^*$ | dC | | |
| $12^1$A | 5.89 | 211 | 0.002 | −12.92 | $n_{c+g} \rightarrow \pi_{g,l}^*$ | dG | | |
| $13^1$A | 5.90 | 210 | 0.001 | 3.95 | $n_{c+g} \rightarrow \pi_{g,l}^*$ | dG | | |
| $14^1$A | 6.44 | 193 | 0.010 | 5.88 | $n_{g+g} \rightarrow \pi_{g,l}^*$ | dG | | |

[a]Excitation energy. [b]Oscillator strength. [c]Rotatory strength ($10^{-40}$ cgs). [d]Subscript *g* and *c* represent guanine and cytosine, respectively. Subscript *h*, *h*−*1*, *l*, and *l*+*1* represent the highest occupied molecular orbital (HOMO), HOMO−1, the lowest unoccupied molecular orbital (LUMO), and LUMO+1 of dG or dC. [e]dG and dC represent the intramolecular excited states of deoxyguanosine and deoxycytidine, respectively. ET(s) represents the electron transfer excited states from guanine to cytosine through the stacking interaction, respectively. [f]Reference 6. [g]Reference 2.

zDNA-L1 model but are opposite to those of the zDNA-L2 model. For the zDNA-L1 model, the first band is assigned to the 1, 2, 3, and $5^1$A excited states with the negative rotatory strength. The lowest two excited states are the electron transfer (ET) excitations from guanine to cytosine through the stacking interaction. The 3 and $5^1$A excited states are the intramolecular excitations of guanine and cytosine, respectively. The second band is assigned to the 8 and $10^1$A excited states of the intramolecular excitations. However, the SAC−CI CD spectrum of the zDNA-L2 model is opposite to the experimental one due to the lowest three excited states with a positive rotatory strength and the $8^1$A excited state with a negative rotatory strength. Despite of the smaller distance between the two base pairs of the zDNA-L2 model than that of the zDNA-L1 model (see Table 1), the stacking ET excited states were calculated at 5.15 and 5.17 eV (6 and $7^1$A), because the overlap between the two base pairs is small (see Figure 2).

For the UV spectra, the shoulder peak at 290 nm is weak for the zDNA-L1 model but strong for the zDNA-L2 model. For the zDNA-L2 model, the intramolecular excited states with the strong oscillator strength are calculated to be at the lower energy (higher wavelength) region and the sum of the oscillator strength of the excited states assigned to the shoulder peak is larger than that of the zDNA-L1 model. However, the main peak at 256 nm is stronger for the zDNA-L1 model, because the sum of the oscillator strength of the excited states assigned to the main peak is larger than that of the zDNA-L2 model. For the zDNA-L2 model, the hydrogen-bonding ET excited states are also calculated at 5.54 and 5.56 eV (10 and $11^1$A). But, they do not contribute to the CD and UV spectra due to the weak intensities.



DOI: 10.1021/acs.jpca.6b08023
J. Phys. Chem. A 2016, 120, 9008−9018

**Table 6. Excited States of bDNA-R2 Model**

| | SAC−CI | | | | | | exptl (eV/nm) | |
|---|---|---|---|---|---|---|---|---|
| state | EE (eV)[a] | EE (nm)[a] | osc[b] | rot[c] | nature[d] | type[e] | CD[f] | UV[g] |
| $1^1$A | 3.76 | 330 | 0.001 | 0.81 | $\pi_{g,h} \rightarrow \pi_{c,l}^*$ | ET(s) | – | |
| $2^1$A | 4.26 | 291 | 0.003 | −3.84 | $\pi_{g,h} \rightarrow \pi_{c,l}^*$ | ET(s) | | |
| $3^1$A | 4.30 | 289 | 0.007 | 1.81 | $\pi_{g,h} \rightarrow \pi_{c,l}^*$ | ET(h) | | |
| $4^1$A | 4.57 | 271 | 0.006 | 3.63 | $\pi_{g,h} \rightarrow \pi_{c,l}^*$ | ET(h) | | |
| $5^1$A | 4.68 | 265 | 0.024 | −1.56 | $\pi_{c,h-1} \rightarrow \pi_{c,l}^*$ | dC | | |
| $6^1$A | 4.82 | 257 | 0.111 | −6.05 | $\pi_{c,h} \rightarrow \pi_{c,l}^*$ | dC | | 4.28/290 |
| $7^1$A | 4.93 | 251 | 0.072 | 52.17 | $\pi_{g,h} \rightarrow \pi_{g,l}^*$ | dG | | |
| $8^1$A | 5.00 | 248 | 0.039 | −40.03 | $\pi_{c,h} \rightarrow \pi_{c,l}^* + \pi_{g,h} \rightarrow \pi_{g,l+1}^*$ | dC + dG | | |
| $9^1$A | 5.09 | 244 | 0.294 | −20.87 | $\pi_{c,h} \rightarrow \pi_{c,l}^* + \pi_{g,h} \rightarrow \pi_{g,l+1}^*$ | dC + dG | | |
| $10^1$A | 5.37 | 231 | 0.210 | −69.14 | $\pi_{c,h-1} \rightarrow \pi_{c,l}^*$ | dC | | 4.84/256 |
| $11^1$A | 5.56 | 223 | 0.156 | 33.66 | $\pi_{g,h} \rightarrow \pi_{g,l}^*$ | dG | | 4.84/256 |
| $12^1$A | 5.61 | 221 | 0.357 | 123.72 | $\pi_{g,h} \rightarrow \pi_{g,l+1}^*$ | dG | | 4.84/256 |
| $13^1$A | 5.71 | 217 | 0.003 | −10.72 | $n_g \rightarrow \pi_{g,l+1}^*$ | dG | | |
| $14^1$A | 6.04 | 205 | 0.002 | 13.94 | $\pi_g \rightarrow \pi_{g,l}^*$ | dG | | |

[a]Excitation energy. [b]Oscillator strength. [c]Rotatory strength ($10^{-40}$ cgs). [d]Subscript *g* and *c* represent guanine and cytosine, respectively. Subscript *h*, *h*−*1*, *l*, and *l*+*1* represent the highest occupied molecular orbital (HOMO), HOMO−1, the lowest unoccupied molecular orbital (LUMO), and LUMO+1 of dG or dC. [e]dG and dC represent the intramolecular excited states of deoxyguanosine and deoxycytidine, respectively. ET(s) and ET(h) represent the electron transfer excited states from guanine to cytosine through the stacking and hydrogen-bonding interactions, respectively. [f]Not assigned. [g]Reference 2.

**Table 7. Excited States of zRNA-L1 Model**

| | SAC−CI | | | | | | exptl (eV/nm) | |
|---|---|---|---|---|---|---|---|---|
| state | EE (eV)[a] | EE (nm)[a] | osc[b] | rot[c] | nature[d] | type[e] | CD[f] | UV[g] |
| $1^1$A | 4.91 | 253 | 0.031 | 52.72 | $\pi_{c,h-1} \rightarrow \pi_{c,l}^*$ | C | 4.37/284 | |
| $2^1$A | 5.07 | 244 | 0.027 | −75.05 | $\pi_{g,h} \rightarrow \pi_{c,l}^*$ | ET(s) | | |
| $3^1$A | 5.10 | 243 | 0.072 | −27.71 | $\pi_{c,h} \rightarrow \pi_{c,l}^*$ | C | | 4.28/290 |
| $4^1$A | 5.14 | 241 | 0.005 | 54.86 | $\pi_{g,h} \rightarrow \pi_{g,l}^* + \pi_{g,h} \rightarrow \pi_{c,l}^*$ | G + ET(s) | 4.70/264 | |
| $5^1$A | 5.21 | 238 | 0.047 | 80.06 | $\pi_{c,h} \rightarrow \pi_{c,l}^*$ | C | 4.70/264 | |
| $6^1$A | 5.28 | 235 | 0.083 | −114.09 | $\pi_{c,h-1} \rightarrow \pi_{c,l}^*$ | C | | |
| $7^1$A | 5.46 | 227 | 0.001 | −7.29 | $n_g \rightarrow \pi_{g,l}^*$ | G | | |
| $8^1$A | 5.54 | 224 | 0.420 | −10.43 | $n_g \rightarrow \pi_{g,l+1}^*$ | G | | 4.86/255 |
| $9^1$A | 5.59 | 222 | 0.296 | 15.54 | $\pi_{c,h-1} \rightarrow \pi_{c,l}^*$ | C | | 4.86/255 |
| $10^1$A | 5.67 | 219 | 0.272 | −13.20 | $n_g \rightarrow \pi_{g,l}^*$ | G | | 4.86/255 |
| $11^1$A | 5.72 | 217 | 0.229 | −25.72 | $\pi_g \rightarrow \pi_{g,l+1}^*$ | G | | 4.86/255 |
| $12^1$A | 5.75 | 216 | 0.064 | 88.30 | $\pi_{c,h-1} \rightarrow \pi_{c,l}^*$ | C | | |
| $13^1$A | 5.82 | 213 | 0.006 | −0.21 | $n_g \rightarrow \pi_{g,l}^*$ | G | | |
| $14^1$A | 5.84 | 212 | 0.065 | −11.83 | $\pi_{g,h} \rightarrow \pi_{c,l}^*$ | ET(h) | | |

[a]Excitation energy. [b]Oscillator strength. [c]Rotatory strength ($10^{-40}$ cgs). [d]Subscript *g* and *c* represent guanine and cytosine, respectively. Subscripts *h*, *h*−*1*, *l*, and *l*+*1* represent the highest occupied molecular orbital (HOMO), HOMO−1, the lowest unoccupied molecular orbital (LUMO), and LUMO+1 of dG or dC. [e]dG and dC represent the intramolecular excited states of deoxyguanosine and deoxycytidine, respectively. ET(s) and ET(h) represent the electron transfer excited states from guanine to cytosine through the stacking and hydrogen-bonding interactions, respectively. [f]Reference 11. [g]Reference 9.

**6.2. B-DNA (Tables 5 and 6).** The experimental CD spectrum is positive for the first band and negative for the second band. For the bDNA-R1 model, the sign of the first band agrees with the experimental one due to the 1 and $3^1$A excited states with the intramolecular excitation nature. However, the second band is positive due to the $9^1$A excited state with the strong oscillator strength. In the experimental UV spectrum, the shoulder and main peaks of the B-DNA appear at the same energies (wavelengths) as those of Z-DNA. However, the shoulder peak of the bDNA-R1 model is stronger than that of the zDNA-L1 model. The hydrogen-bonding interaction shifts the excitation energies to the higher energy region as compared with those of monomers (dG or dC).[14] Since the angles between the two bases are lager for the bDNA-R1 model than for the zDNA-L1 model (see Table 2), the excited states of the bDNA-R1 model are closer to those of the monomers than those of the zDNA-L1 model. Therefore, the shoulder peak of the bDNA-R1 model is stronger and calculated to be at a lower energy region than that of the zDNA-L1 model.

For the bDNA-R2 model, the 1 and $2^1$A excited states are the stacking ET excitation and the 3 and $4^1$A excited states are the hydrogen-bonding ET excitation. However, their oscillator and rotatory strengths are weak. Since the excitation energies are lower than those of the other models due to the unstable ground state, both SAC−CI UV and CD spectra are much different from the experimental spectra of B-DNA.

**6.3. Z-RNA (Tables 7 and 8).** The experimental CD spectrum is positive for both of the first and second bands. However, the SAC−CI CD spectra of both zRNA-L1 and zRNA-L2 models disagree with the experimental one. For the



DOI: 10.1021/acs.jpca.6b08023
J. Phys. Chem. A 2016, 120, 9008−9018

**Table 8. Excited States of zRNA-L2 Model**

| | SAC−CI | | | | | | exptl (eV/nm) | |
|---|---|---|---|---|---|---|---|---|
| state | EE (eV)[a] | EE (nm)[a] | osc[b] | rot[c] | nature[d] | type[e] | CD[f] | UV[g] |
| $1^1$A | 4.55 | 273 | 0.004 | −6.80 | $\pi_{g,h} \rightarrow \pi_{c,l}^*$ | ET(s) | − | |
| $2^1$A | 4.64 | 267 | 0.008 | −13.23 | $\pi_{g,h} \rightarrow \pi_{c,l}^*$ | ET(s) | | |
| $3^1$A | 4.91 | 252 | 0.094 | 25.08 | $\pi_{c,h} \rightarrow \pi_{c,l}^*$ | C | | 4.28/290 |
| $4^1$A | 5.00 | 248 | 0.063 | −28.48 | $\pi_{c,h} \rightarrow \pi_{c,l}^*$ | C | | |
| $5^1$A | 5.23 | 237 | 0.021 | 15.55 | $\pi_{c,h-1} \rightarrow \pi_{c,l}^* + \pi_{g,h} \rightarrow \pi_{g,l}^*$ | C + G | | |
| $6^1$A | 5.28 | 235 | 0.012 | −63.43 | $\pi_{c,h-1} \rightarrow \pi_{c,l}^*$ | C | | |
| $7^1$A | 5.29 | 234 | 0.045 | −25.18 | $\pi_{g,h} \rightarrow \pi_{g,l}^*$ | G | | |
| $8^1$A | 5.37 | 231 | 0.002 | −1.37 | $n_c \rightarrow \pi_{c,l}^*$ | C | | |
| $9^1$A | 5.45 | 227 | 0.554 | 95.46 | $\pi_{g,h} \rightarrow \pi_{g,l}^* + \pi_{c,h-1} \rightarrow \pi_{c,l}^*$ | G + C | | 4.86/255 |
| $10^1$A | 5.56 | 223 | 0.005 | −20.45 | $n_g \rightarrow \pi_{g,l}^*$ | G | | |
| $11^1$A | 5.64 | 220 | 0.564 | 248.74 | $\pi_{g,h} \rightarrow \pi_{g,l+1}^*$ | G | | 4.86/255 |
| $12^1$A | 5.66 | 219 | 0.021 | −30.28 | $n_c \rightarrow \pi_{c,l}^*$ | C | | |
| $13^1$A | 5.67 | 218 | 0.191 | −262.24 | $\pi_{g,h} \rightarrow \pi_{g,l+1}^*$ | G | | 4.86/255 |
| $14^1$A | 5.72 | 217 | 0.001 | −6.96 | $n_g \rightarrow \pi_{g,l}^*$ | G | | |

[a]Excitation energy. [b]Oscillator strength. [c]Rotatory strength ($10^{-40}$ cgs). [d]Subscript *g* and *c* represent guanine and cytosine, respectively. Subscript *h*, *h*−*1*, *l* and *l*+*1* represent the highest occupied molecular orbital (HOMO), HOMO−1, the lowest unoccupied molecular orbital (LUMO), and LUMO+1 of dG or dC. [e]dG and dC represent the intramolecular excited states of deoxyguanosine and deoxycytidine, respectively. ET(s) represents the electron transfer excited states from guanine to cytosine through the stacking interaction. [f]Not assigned. [g]Reference 9.

**Table 9. Excited States of aRNA-R1 Model**

| | SAC−CI | | | | | | exptl (eV/nm) | |
|---|---|---|---|---|---|---|---|---|
| state | EE (eV)[a] | EE (nm)[a] | osc[b] | rot[c] | nature[d] | type[e] | CD[f] | UV[g] |
| $1^1$A | 4.52 | 274 | 0.006 | −31.19 | $\pi_{g,h} \rightarrow \pi_{c,l}^*$ | ET(s) | 4.22/294 | |
| $2^1$A | 4.61 | 269 | 0.008 | −36.45 | $\pi_{g,h} \rightarrow \pi_{c,l}^*$ | ET(s) | 4.22/294 | |
| $3^1$A | 5.23 | 237 | 0.043 | −60.20 | $\pi_{c,h} \rightarrow \pi_{c,l}^* + \pi_{g,h} \rightarrow \pi_{g,l}^*$ | C + G | | |
| $4^1$A | 5.25 | 236 | 0.054 | 72.79 | $\pi_{g,h} \rightarrow \pi_{g,l}^*$ | G | 4.64/267 | |
| $5^1$A | 5.28 | 235 | 0.025 | 105.04 | $\pi_{c,h} \rightarrow \pi_{c,l}^*$ | C | 4.64/267 | |
| $6^1$A | 5.39 | 230 | 0.049 | −149.29 | $\pi_{c,h-1} \rightarrow \pi_{c,l}^*$ | C | | |
| $7^1$A | 5.50 | 225 | 0.620 | 273.00 | $\pi_{c,h-1} \rightarrow \pi_{c,l}^*$ | C | 4.64/267 | 4.81/258 |
| $8^1$A | 5.62 | 221 | 0.798 | −256.15 | $\pi_{g,h} \rightarrow \pi_{g,l}^*$ | G | | 4.81/258 |
| $9^1$A | 5.66 | 219 | 0.012 | 65.54 | $\pi_{g,h} \rightarrow \pi_{g,l+1}^*$ | G | | |
| $10^1$A | 5.91 | 210 | 0.002 | −0.29 | $n_c \rightarrow \pi_{c,l}^*$ | C | | |
| $11^1$A | 5.92 | 210 | 0.003 | 4.99 | $n_c \rightarrow \pi_{c,l}^*$ | C | | |
| $12^1$A | 6.07 | 204 | 0.001 | 2.56 | $n_g \rightarrow \pi_{g,l}^*$ | G | | |
| $13^1$A | 6.15 | 202 | 0.001 | 10.96 | $n_g \rightarrow \pi_{g,l}^*$ | G | | |
| $14^1$A | 6.90 | 180 | 0.013 | −2.50 | $\pi_{g,h} \rightarrow \pi_{g,l+1}^*$ | G | | |

[a]Excitation energy. [b]Oscillator strength. [c]Rotatory strength ($10^{-40}$ cgs). [d]Subscript *g* and *c* represent guanine and cytosine, respectively. Subscript *h*, *h-1*, *l* and *l+1* represent the highest occupied molecular orbital (HOMO), HOMO−1, the lowest unoccupied molecular orbital (LUMO), and LUMO+1 of G or C. [e]G and C represent the intramolecular excited states of guanosine and cytidine, respectively. ET(s) represents the electron transfer excited states from guanine to cytosine through the stacking interaction. [f]Reference 11. [g]Reference 9.

zRNA-L1 model, the first band is positive due to the $1^1$A excited state, but the second band is negative due to the 2 and $6^1$A excited states. For the zRNA-L2 model, the SAC−CI CD spectrum is quite different from the experimental one. Only the sign of the first band of the zRNA-L1 model is the same as the sign of the experimental CD spectrum. As explained in section 2, "Modeling", the zRNA-L2 model has the strong stacking interaction as seen from the small angles and the large overlap between the two bases (see Table 2 and Figure 2). Therefore, the lowest two excited states (1 and $2^1$A) of the zRNA-L2 model is the stacking ET excitation with a negative rotatory strength, similarly to the zDNA-L1 and aRNA-R1 models. However, their intensities are weak and the $3^1$A excited state with the intramolecular excitation has a positive rotatory strength. Therefore, in the SAC−CI CD spectrum of the zRNA-L2 model, the negative peak at 295 nm is weak.

The SAC−CI UV spectra are similar between the zRNA-L1 and zRNA-L2 models. Both SAC−CI UV spectra have the main and shoulder peaks and agree with the experimental one. However, the main peak is composed of four excited states for the zRNA-L1 model but three excited states for the zRNA-L2 model.

**6.4. A-RNA (Tables 9 and 10).** The experimental CD spectrum is negative for the first band and positive for the second band. The features are the same as those of Z-DNA. For the aRNA-R1 model, the lowest two excited states (1 and $2^1$A) are the stacking ET excitation with the negative rotatory strength. The main peak is assigned to the 4, 5 and $7^1$A excited states, which are the intramolecular excitations with the positive rotatory strengths. These are the same as those of the zDNA-L1 model. However, for the aRNA-R2 model, the lowest four excited states are the intramolecular excitations, because the angle between the two bases is large (see Table 2) and the



DOI: 10.1021/acs.jpca.6b08023
J. Phys. Chem. A 2016, 120, 9008−9018

Table 10. Excited States of aRNA-R2 Model

| | SAC−CI | | | | | | exptl (eV/nm) | |
|---|---|---|---|---|---|---|---|---|
| state | EE (eV)[a] | EE (nm)[a] | osc[b] | rot[c] | nature[d] | type[e] | CD[f] | UV[g] |
| $1^1$A | 4.90 | 253 | 0.046 | 19.55 | $\pi_{c,h} \rightarrow \pi_{c,l}^*$ | C | − | |
| $2^1$A | 4.91 | 252 | 0.204 | 37.56 | $\pi_{c,h} \rightarrow \pi_{c,l}^*$ | C | | |
| $3^1$A | 4.93 | 251 | 0.013 | 1.93 | $\pi_{g,h} \rightarrow \pi_{g,l}^*$ | G | | |
| $4^1$A | 5.01 | 247 | 0.054 | −29.64 | $\pi_{g,h} \rightarrow \pi_{g,l}^*$ | G | | |
| $5^1$A | 5.13 | 242 | 0.001 | −5.32 | $\pi_{g,h} \rightarrow \pi_{c,l}^*$ | ET(s) | | |
| $6^1$A | 5.22 | 237 | 0.057 | 115.94 | $\pi_{c,h-1} \rightarrow \pi_{c,l}^*$ | C | | |
| $7^1$A | 5.31 | 233 | 0.248 | −255.16 | $\pi_{c,h-1} \rightarrow \pi_{c,l}^* + \pi_{g,h} \rightarrow \pi_{c,l}^*$ | C + ET(s) | | 4.81/258 |
| $8^1$A | 5.36 | 231 | 0.078 | 2.49 | $\pi_{g,h} \rightarrow \pi_{c,l}^* + \pi_{c,h-1} \rightarrow \pi_{c,l}^*$ | ET(s) + C | | |
| $9^1$A | 5.59 | 222 | 0.295 | 191.74 | $\pi_{g,h} \rightarrow \pi_{g,l+1}^*$ | G | | 4.81/258 |
| $10^1$A | 5.69 | 218 | 0.734 | −10.41 | $\pi_{g,h} \rightarrow \pi_{c,l}^* + \pi_{g,h} \rightarrow \pi_{g,l}^*$ | ET(h) + G | | 4.81/258 |
| $11^1$A | 5.77 | 215 | 0.002 | 1.63 | $n_g \rightarrow \pi_{g,l}^* + n_c \rightarrow \pi_{c,l}^*$ | G + C | | |
| $12^1$A | 5.81 | 213 | 0.000 | 0.36 | $n_c \rightarrow \pi_{c,l}^* + n_g \rightarrow \pi_{g,l}^*$ | C + G | | |
| $13^1$A | 5.87 | 211 | 0.002 | 3.24 | $n_c \rightarrow \pi_{c,l}^* + \pi_{g,h} \rightarrow \pi_{c,l}^*$ | C + ET(h) | | |
| $14^1$A | 6.07 | 204 | 0.001 | 5.80 | $n_g \rightarrow \pi_{g,l}^*$ | G | | |

[a]Excitation energy. [b]Oscillator strength. [c]Rotatory strength ($10^{-40}$ cgs). [d]Subscript *g* and *c* represent guanine and cytosine, respectively. Subscript *h*, *h*−*1*, *l* and *l*+*1* represent the highest occupied molecular orbital (HOMO), HOMO−1, the lowest unoccupied molecular orbital (LUMO), and LUMO+1 of dG or dC. [e]dG and dC represent the intramolecular excited states of deoxyguanosine and deoxycytidine, respectively. ET(s) and ET(h) represent the electron transfer excited states from guanine to cytosine through the stacking and hydrogen-bonding interactions, respectively. [f]Not assigned. [g]Reference 9.

overlap between the two base pairs is small (see Figure 2). The first band is positive due to the 1 and $2^1$A excited states. The lowest stacking ET excited state ($5^1$A) has the weak oscillator and rotatory strengths. The second band is negative due to the $7^1$A excited state with the intramolecular excitation of cytosine and the stacking ET excitation. The hydrogen-bonding ET excitation is calculated at 5.69 and 5.87 eV (10 and $13^1$A). The features of the excited states of the aRNA-R2 model are similar to those of the zDNA-L2 model.

The SAC−CI UV spectrum of the aRNA-R1 model is in good agreement with the experimental UV spectrum. However, the UV spectrum of the aRNA-R2 model has a shoulder peak due to the $2^1$A excited state with the strong oscillator strength. Since the aRNA-R2 model has the large angles between the two bases, the hydrogen-bonding and stacking interactions are weak. Therefore, the features of the excited states are close to those of the monomers.[14] Thus, the shoulder peak may be observed in the UV spectra of DNA and RNA by the large inclination between the two bases.

**6.5. Comparison of CD Spectra.** For the zDNA-L1 and aRNA-R1 models, the lowest two excited states are the stacking electron transfer (ET) excitation from guanine to cytosine and their rotatory strengths have a negative sign. These excited states are the origin of the negative peak at 295 nm of CD spectra of Z-DNA and A-RNA. For the bDNA-R2 and zRNA-L2 models, the lowest excited state is also the ET excitation. However, for the bDNA-R2 model, the rotatory strengths of the lowest four ET excited states are very weak and only one excited state among them has a negative sign. For the zRNA-L2 model, the rotatory strength of the lowest two ET excited states is weak and the $3^1$A excited state has a positive rotatory strength. Therefore, the strong negative peak at 295 nm is not observed in the CD spectra of B-DNA and Z-RNA. On the other hand, for the zDNA-L2, bDNA-R1, zRNA-L1, and aRNA-R2 models, the lowest excited states are the intramolecular excitation with the positive rotatory strength, not the ET excitation. Thus, when the two bases are approximately parallel to each other and the overlap between the two bases is large, the lowest two excited states become the ET excitation due to the strong stacking interaction, which is the origin of the negative peak of the CD spectra of both DNA and RNA.

**6.6. Comparison of UV Spectra.** For the Z-DNA and Z-RNA, the SAC−CI UV spectra have the shoulder peak, similarly to the experimental UV spectra. In the experimental UV spectra, the shoulder peak is not observed for A-RNA and is weak for B-DNA. However, the SAC−CI UV spectra have the shoulder peak for the bDNA-R1, bDNA-R2, and aRNA-R2 models except for the aRNA-R1 model. For the bDNA-R1 and aRNA-R2 models, the lowest two excited states are the intramolecular excitations, but the angles between the two bases are large (see Table 2). Therefore, the intramolecular excitations are calculated to be in the lower region due to the weak hydrogen-bonding interaction.[14] For the bDNA-R2 model, since the ground state is unstable, its excitation energies were calculated to be in the lower energy region than those of the other models. For the aRNA-R1 model, since the lowest two excited states are the stacking ET excitation, their oscillator strengths are weak, only the SAC−CI UV spectrum of the aRNA-R1 model does not have the shoulder peak, similarity to the experimental one.

## 7. CONCLUSION

The features of the observed CD spectra of DNA are opposite to those of RNA: the CD spectrum of the left-handed double-helical Z-DNA is similar to that of the right-handed double-helical A-RNA. We have elucidated the similarities and differences between the CD spectra of DNA and RNA using the tetramer models with the ChiraSac methodology based on the SAC−CI method. Since each DNA or RNA includes two kinds of the stacking interaction between the two base pairs (see Figure 1), we calculated the SAC−CI spectra of the two tetramer models for each DNA and RNA. The SAC−CI spectra of the model-1 (zDNA-L1, bDNA-R1, zRNA-L1, and aRNA-R1) reproduced the signs at 295 nm of the experimental CD spectra of DNA and RNA, but the SAC−CI spectra of the model-2 (zDNA-L2, bDNA-R2, zRNA-L2, and aRNA-R2) did not agree with the experimental one. This showed that the


DOI: 10.1021/acs.jpca.6b08023
J. Phys. Chem. A 2016, 120, 9008−9018

observed CD spectra reflect the geometries and interactions described by the model-1.

The origin of the negative peak at 295 nm of the CD spectra is due to the stacking ET excitation in the model 1 (zDNA-L1 and aRNA-R1). Even if we calculate the large model that includes all interactions in both models 1 and 2, we expect that the stacking ET excited states due to the model 2 do not appear at 295 nm of the SAC−CI CD spectra, because the stacking ET excited states are calculated to be in a higher energy region for the model 2 (zDNA-L2 and aRNA-R2) (see Tables 4 and 10). Therefore, we can conclude that the negative peak at 295 nm is the indicator of the stacking interaction in the double-helical structures of both DNA and RNA.

## ■ ASSOCIATED CONTENT

### Supporting Information

The Supporting Information is available free of charge on the ACS Publications website at DOI: 10.1021/acs.jpca.6b08023.

Coordinates of eight tetramer models (PDF)

## ■ AUTHOR INFORMATION


### Corresponding Author

*(H.N.) E-mail: h.nakatsuji@qcri.or.jp. Telephone: +81-75-634-3211. Fax: +81-75-634-3211.


### Notes

The authors declare no competing financial interest.

## ■ ACKNOWLEDGMENTS

The computations were carried out using the computers at the Research Center for Computational Science, Okazaki, Japan, whom we acknowledge sincerely. We also thank the support of Mr. Nobuo Kawakami for the researches of QCRI. This work was supported by JSPS KAKENHI Grant Numbers 15K05408.

## ■ REFERENCES


(1) Rich, A.; Nordheim, A.; Wang, A. H.-J. The Chemistry and Biology of Left-Handed Z-DNA. *Annu. Rev. Biochem.* **1984**, *53*, 791−846.

(2) Tran-Dinh, S.; Taboury, J.; Neumann, J.-M.; Huynh-Dinh, T.; Genissel, B.; Langlois d'Estaintot, B.; Igolen, J. $^{1}$H NMR and Circular Dichroism Studies of the B and Z Conformations of the Self-Complementary Deoxyhexanucleotide d(m$^{5}$C-G-C-G-m$^{5}$C-G): Mechanism of the Z-B-Coil Transitions. *Biochemistry* **1984**, *23*, 1362−1371.

(3) Sugiyama, H.; Kawai, K.; Matsunaga, A.; Fujimoto, K.; Saito, I.; Robinson, H.; Wang, A. H.-J. Synthesis, structure and thermodynamic Properties of 8-methylguanine-containing oligonucleotides: Z-DNA under physiological salt conditions. *Nucleic Acids Res.* **1996**, *24*, 1272−1278.

(4) Kawai, K.; Saito, I.; Sugiyama, H. Conformation Dependent Photochemistry of 5-Halouracil-Containing DNA: Stereospecific 2′$\alpha$-Hydroxylation of Deoxyribose in Z-form DNA. *J. Am. Chem. Soc.* **1999**, *121*, 1391−1392.

(5) Oyoshi, T.; Kawai, K.; Sugiyama, H. Efficient C2′$\alpha$-Hydroxylation of Deoxyribose in Protein-Induced Z-Form DNA. *J. Am. Chem. Soc.* **2003**, *125*, 1526−1531.

(6) Xu, Y.; Ikeda, R.; Sugiyama, H. 8-Methylguanosine: A Powerful Z-DNA Stabilizer. *J. Am. Chem. Soc.* **2003**, *125*, 13519−13524.

(7) *Circular Dichroism: Principles and Applications*; Berova, N., Nakanishi, K., Woody, R. W., Eds; Wiley-VCH: New York, 2000.

(8) *Comprehensive Chiroptical Spectroscopy*; Berova, N., Polavarapu, P. L., Nakanishi, K., Woody, R. W., Eds; Wiley: Hoboken, NJ, 2012; Vol. 2.

(9) Hall, K.; Cruz, P.; Tinoco, I., Jr.; Jovin, T. M.; van de Sande, J. H. 'Z-RNA'—a left-handed RNA double helix. *Nature* **1984**, *311*, 584−586.

(10) Brown, B. A., II; Lowenhaupt, K.; Wilbert, C. M.; Hanlon, E. B.; Rich, A. The Z$\alpha$ domain of the editing enzyme dsRNA adenosine deaminase binds left-handed Z-RNA as well as Z-DNA. *Proc. Natl. Acad. Sci. U. S. A.* **2000**, *97*, 13532−13536.

(11) Tashiro, R.; Sugiyama, H. Biomolecule-Based Switching Devices that Respond Inversely to Thermal Stimuli. *J. Am. Chem. Soc.* **2005**, *127*, 2094−2097.

(12) Nielsen, L. M.; Holm, A. I. S.; Varsano, D.; Kadhane, U.; Hoffmann, S. V.; Di Felice, R.; Rubio, A.; Nielsen, S. B. Fingerprints of Bonding Motifs in DNA Duplexes of Adenine and Thymine Revealed from Circular Dichroism: Synchrotron Radiation Experiments and TDDFT Calculations. *J. Phys. Chem. B* **2009**, *113*, 9614−9619.

(13) Di Meo, F.; Pedersen, M. N.; Rubio-Magnieto, J.; Surin, M.; Linares, M.; Norman, P. DNA Electronic Circular Dichroism on the Inter-Base Pair Scale: An Experimental−Theoretical Case Study of the AT Homo-Oligonucleotide. *J. Phys. Chem. Lett.* **2015**, *6*, 355−359.

(14) Miyahara, T.; Nakatsuji, H.; Sugiyama, H. Helical Structure and Circular Dichroism Spectra of DNA: A Theoretical Study. *J. Phys. Chem. A* **2013**, *117*, 42−55.

(15) Miyahara, T.; Nakatsuji, H. Indicator of the Stacking Interaction in the DNA Double-Helical Structure: ChiraSac Study. *J. Phys. Chem. A* **2015**, *119*, 8269−8278.

(16) Miyahara, T.; Nakatsuji, H. Conformational Dependence of the Circular Dichroism Spectra of $\alpha$-Hydroxyphenylacetic Acid: A ChiraSac study. *J. Phys. Chem. A* **2013**, *117*, 14065−14074.

(17) Miyahara, T.; Nakatsuji, H.; Wada, T. Circular Dichroism Spectra of Uridine Derivatives: ChiraSac Study. *J. Phys. Chem. A* **2014**, *118*, 2931−2941.

(18) Nakatsuji, H.; Hirao, K. Cluster Expansion of the Wavefunction. Symmetry-Adapted-Cluster Expansion, Its Variational Determination, and Extension of Open-Shell Orbital Theory. *J. Chem. Phys.* **1978**, *68*, 2053−2065.

(19) Nakatsuji, H. Cluster Expansion of the Wavefunction. Excited States. *Chem. Phys. Lett.* **1978**, *59*, 362−364.

(20) Nakatsuji, H. Cluster Expansion of the Wavefunction. Electron Correlations in Ground and Excited States by SAC (Symmetry-Adapted-Cluster) and SAC-CI Theories. *Chem. Phys. Lett.* **1979**, *67*, 329−333.

(21) Nakatsuji, H. Cluster Expansion of the Wavefunction. Calculation of Electron Correlations in Ground and Excited States by SAC and SAC-CI Theories. *Chem. Phys. Lett.* **1979**, *67*, 334−342.

(22) Nakatsuji, H. Electronic Structures of Ground, Excited, Ionized, and Anion States Studied by the SAC/SAC-CI Theory. *Acta Chim. Hung. Models in Chemistry* **1992**, *129*, 719−776.

(23) Nakatsuji, H.; SAC-CI Method: Theoretical Aspects and Some Recent Topics. In *Computational Chemistry − Reviews of Current Trends*; Leszczynski, J., Ed.; World Scientific: Singapore, 1997; Vol. 2, pp 62−124.

(24) Nakatsuji, H. Deepening and Extending the Quantum Principles in Chemistry. *Bull. Chem. Soc. Jpn.* **2005**, *78*, 1705−1724.

(25) Ehara, M.; Hasegawa, J.; Nakatsuji, H. SAC-CI Method Applied to Molecular Spectroscopy. In *Theory and Applications of Computational Chemistry: The First 40 Years, A Vol. of Technical and Historical Perspectives*; Dykstra, C. E., Frenking, G., Kim, K. S., Scuseria, G. E., Eds.; Elsevier: Oxford, U.K., 2005; pp 1099−1141.

(26) Hasegawa, J., Nakatsuji, H. Exploring Photo-Biology and Bio-Spectroscopy with the SAC-CI (Symmetry-Adapted Cluster-Configuration Interaction) Method, In *Radiation Induced Molecular Phenomena in Nucleic Acid: A Comprehensive Theoretical and Experimental Analysis, by*; Shukla, M., Leszczynsk, J., Eds., Springer: 2008, Chapter 4, 93−124.

(27) Frisch, M. J.; Trucks, G. W.; Schlegel, H. B.; Scuseria, G. E.; Robb, M. A.; Cheeseman, J. R.; Scalmani, G.; Barone, V.; Mennucci, B.; Petersson, G. A.; et al. *Gaussian 09*; Gaussian, Inc.: Wallingford CT, 2009.




DOI: 10.1021/acs.jpca.6b08023
J. Phys. Chem. A 2016, 120, 9008−9018

(28) Becke, A. D. Density-functional thermochemistry. III. The role of exact exchange. *J. Chem. Phys.* **1993**, *98*, 5648−5652.
(29) Lee, C.; Yang, W.; Parr, R. G. Development of the Colle-Salvetti correlation-energy formula into a functional of the electron density. *Phys. Rev. B: Condens. Matter Mater. Phys.* **1988**, *37*, 785−789.
(30) Hariharan, P. C.; Pople, J. A. Influence of polarization functions on molecular-orbital hydrogenation energies. *Theor. Chim. Acta* **1973**, *28*, 213−222.
(31) Francl, M. M.; Pietro, W. J.; Hehre, W. J.; Binkley, J. S.; Gordon, M. S.; DeFrees, D. J.; Pople, J. A. Self-Consistent Molecular Orbital Methods. 23. A polarization-type basis set for 2nd-row elements. *J. Chem. Phys.* **1982**, *77*, 3654−3665.
(32) Dunning, T. H., Jr.; Hay, P. J. In *Modern Theoretical Chemistry*; Schaefer, H. F., III., Ed.; Plenum: New York, 1976; Vol. *3*, pp 1−28.
(33) Nakatsuji, H. Cluster Expansion of the Wavefunction. Valence and Rydberg Excitations, Ionizations, and Inner-Valence Ionizations of $CO_2$ and $N_2O$ Studied by the SAC and SAC-CI Theories. *Chem. Phys.* **1983**, *75*, 425−441.



DOI: 10.1021/acs.jpca.6b08023
*J. Phys. Chem. A* 2016, 120, 9008−9018